



Contents lists available at SciVerse ScienceDirect

Bioorganic & Medicinal Chemistry Letters

journal homepage: www.elsevier.com/locate/bmcl

Highly selective 2,4-diaminopyrimidine-5-carboxamide inhibitors of Sky kinase

Noel A. Powell^{*}, Jennifer K. Hoffman[†], Fred L. Ciske[‡], Michael D. Kaufman[§], Jeffrey T. Kohrt[¶], John Quin III, Derek J. Sheehan^{||}, Amy Delaney, Sangita M. Baxi^{††}, Cornel Catana, Patrick McConnell, Jeff Ohren, Lisa A. Perrin, Jeremy J. Edmunds^{‡‡}

Pfizer Global Research & Development, Michigan Laboratories, Ann Arbor, MI 48105, USA

ARTICLE INFO

Article history:

Available online 20 December 2012

Keywords:

Kinase Inhibitor
Anti-platelet therapy
Hit-to-lead

ABSTRACT

We report the SAR around a series of 2,4-diaminopyrimidine-5-carboxamide inhibitors of Sky kinase. 2-Aminophenethyl analogs demonstrate excellent potency but moderate kinase selectivity, while 2-aminobenzyl analogs that fill the Ala571 subpocket exhibit good inhibition activity and excellent kinase selectivity.

© 2012 Elsevier Ltd. All rights reserved.

Coronary heart disease is the leading cause of mortality and morbidity in the United States.¹ There are an estimated 40 million people in the US at risk for thrombotic events due to atherosclerosis or prior history of cardiovascular disease or stroke. The current front-line treatment for arterial thrombosis is clopidogrel (Plavix[®]), which has significant limitations in terms of efficacy without aspirin, and is also a pro-drug that must be metabolized by liver enzymes to present a pharmacodynamic effect. About one quarter to one third of patients do not adequately metabolize clopidogrel and are resistant to its effect.² In addition, the active drug binds irreversibly to platelets, resulting in a high risk for increased bleeding. Thus, there is a need for safer, more effective anti-platelet agents useful to a broad patient population.

Gas6 (growth arrest specific gene 6) is a member of the Vitamin K dependent family of proteins which have all been shown to have a role in thrombosis and hemostasis.³ Deficiency or inhibition of Gas6 causes platelet dysfunction and protects mice against

thrombosis.^{4,5} Mechanistically, Gas6 appears to play a critical role as a platelet response amplifier, enhancing platelet aggregation and granule secretion to known endogenous agonists. Gas6 is a ligand for three tyrosine kinase receptors designated Sky (Tyro3/Rse), Axl, and Mer that are expressed on human and mouse platelets,⁵ and induces intracellular signaling through the PI3K and Akt pathways.⁶ Gas6-neutralizing antibodies inhibit platelet aggregation, without increased bleeding in mice.⁵ In addition, Gas6 knockout mice do not have any significant difference in bleeding time compared to wild type animals.⁴ Gas6 receptor knockout (Sky^{-/-}, Axl^{-/-}, or Mer^{-/-}) mice also exhibit protection against thromboembolism with normal bleeding times.⁷ Previous studies from our laboratories have demonstrated that Sky specific antibodies inhibit human platelet degranulation and aggregation to the same extent as Gas6 inhibition, and result in comparable efficacy to clopidogrel treatment in a mouse model of thrombosis with no significant increase in bleeding time.⁵ Thus, inhibition of Sky potentially represents the first antithrombotic therapy that is not associated with bleeding side effects.

We recently described the discovery of a spiroindoline-based series of Sky kinase inhibitors that exhibited excellent selectivity against a panel of 30 kinases designed to broadly represent the kinome.⁸ However, that series suffered from poor oral bioavailability and CYP2D6 inhibition. Consequently we were interested in identifying additional chemical matter with improved properties. Compound **1** was identified from a HTS of the Pfizer compound library as a potential lead that exhibited no inhibition of dofetilide binding in the hERG K⁺ channel. In addition, although 2,4-diaminopyrimidine-5-carboxamides are well precedented kinase inhibitor templates, the 3-aminopropyl-butyrolactam sidechain appeared to

^{*} Corresponding author at present address: Eisai Inc., 4 Corporate Drive, Andover, MA 01810, USA. Tel.: +1 978 837 4683.

E-mail address: napowell@comcast.net (N.A. Powell).

[†] Current address: Hamilton Company, 4970 Energy Way, Reno, NV 89502, USA.

[‡] Current address: Cayman Chemical, 1180 East Ellsworth Road, Ann Arbor, MI 48108, USA.

[§] Current address: Deciphera Pharmaceuticals, LLC 643 Massachusetts, Ste 200, Lawrence, KS 66044, USA.

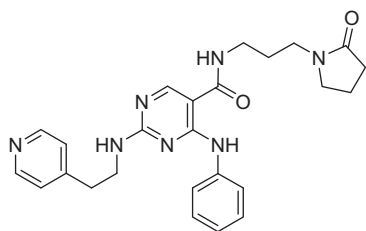
[¶] Current address: Pfizer Worldwide Research & Development, Eastern Point Road, Groton, CT 06340, USA.

^{||} Current address: Pfizer Animal Health, Kalamazoo, MI 49007, USA.

^{††} Current address: Pfizer Worldwide Research & Development, 10646 Science Center Drive, San Diego, CA 92121, USA.

^{‡‡} Current address: Abbott Labs, 381 Plantation Street, Worcester, MA 01605, USA.

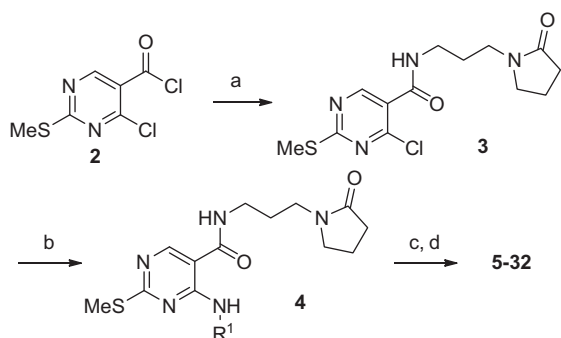
confer some kinase selectivity, as **1** exhibited little activity in several other internal kinase high throughput screens (data not shown). As selectivity against the broader kinome is a paramount concern for a non-oncology kinase inhibitor, we chose to pursue further structure–activity relationship (SAR) studies around this template.



1
Sky IC₅₀ = 1.90 μM
Dofetilide Binding = 6% @ 10 μM

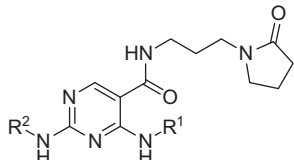
Analogs were prepared as described in Scheme 1. Condensation of *N*-(3-aminopropyl)-butyrolactam with acid chloride **2**⁹ provided the amide **3**. The chloride was displaced by an amine (R¹NH₂) in hot CH₃CN to afford **4**. After *m*-CPBA oxidation of the thiomethyl group to the methyl sulfone, displacement of the sulfone by a second primary amine (R²NH₂) in refluxing 1,4-dioxane yielded the desired 2,4-diaminopyrimidine analogs.

Our initial SAR efforts began by investigating the role of the nitrogen atom in the pyridine ring of the R² sidechain (Table 1). The 3- and 2-pyridine rings exhibited two and threefold less Sky inhibition activity (**5** and **6**, IC₅₀ = 4.2 and 7.2 μM, respectively), indicating that the 4-pyridine **1** makes a positive hydrogen-bond accepting interaction. Recognizing that the aniline moiety in the R¹ sidechain represented a potential toxicophore, we were pleased to find that replacement of the aniline ring with a cyclopentylamine resulted in a slight increase in inhibition activity (**7**, IC₅₀ = 1.1 μM). While our initial SAR indicated that the 4-pyridine nitrogen atom made a positive hydrogen-bond acceptor interaction, a phenethyl group resulted in similar activity (**8**, IC₅₀ = 0.811 μM). Addition of an *R*-methyl substituent at the benzylic position of the phenethyl group resulted in similar activity (**9**, IC₅₀ = 1.1 μM), while a *S*-methyl substituted afforded a twofold loss of activity (**10**, IC₅₀ = 1.95). Constraining the conformational flexible phenethyl moiety into a 2-aminoindane gave a substantial improvement in the Sky inhibition activity (**11**, IC₅₀ = 0.26 μM). Likewise, addition of electron withdrawing substituents on the phenyl ring also led to improved Sky inhibition (**12–15**). The importance of a potential hydrogen-bond acceptor on the phenyl ring was also illustrated by the improved inhibition activity exhibited by the 4-methoxyphenethyl analog **16** (IC₅₀ = 0.20 μM) and



Scheme 1. (a) *N*-(3-Aminopropyl)-butyrolactam, Et₃N, DMAP, CH₂Cl₂; (b) R¹NH₂, Et₃N, CH₃CN, 80 °C; (c) *m*-CPBA, CH₂Cl₂, 0 °C; (d) R²NH₂, Et₃N, 1,4-dioxane, reflux.

Table 1
SAR of 2,4-diaminopyrimidine-5-carboxamide series



ID	R ¹ -NH	R ² -NH	Sky IC ₅₀ ^a (μM)
1	HN-	HN-	1.9
5	HN-	HN-	4.2
6	HN-	HN-	7.2
7	HN-	HN-	1.1
8	HN-	HN-	0.81
9	HN-	HN-	1.1
10	HN-	HN-	2.0
11	HN-	HN-	0.26
12	HN-	HN-	0.11
13	HN-	HN-	0.18
14	HN-	HN-	0.17
15	HN-	HN-	0.36
16	HN-	HN-	0.20
17	HN-	HN-	0.037
18	HN-	HN-	0.27
19	HN-	HN-	0.068
20	HN-	HN-	0.035

^a IC₅₀ data is an average of duplicate runs using an ELISA format assay with ATP concentration of 60 μM.

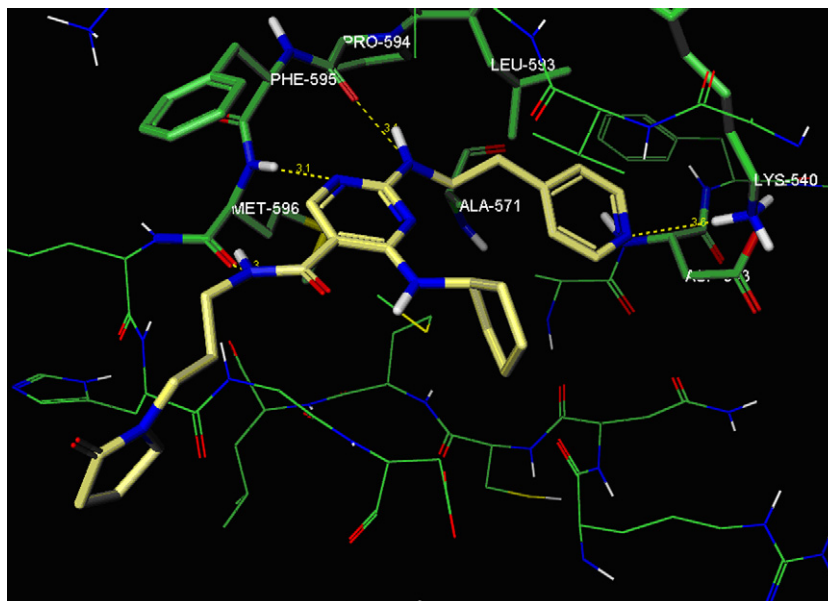


Figure 1. X-ray crystal structure of **7** (yellow stick) bound in the ATP active site of Sky (pdb ID code: 4FEQ). ¹⁰ Dotted lines denote hydrogen bonds formed with protein residues. The glycine-rich loop has been removed for clarity.

the 3-methoxyphenethyl analog **17** ($IC_{50} = 0.037 \mu M$). The combination of the 3,4-dimethoxyphenethyl proved to be less active than the single substituents (**18**, $IC_{50} = 0.27 \mu M$). Since methoxy ethers are potential sites of metabolism, we examined the potential phenol metabolite and found that the 4-hydroxyphenethyl analog **19** exhibited potent Sky inhibition activity ($IC_{50} = 0.068 \mu M$). Unlike the 3,4-dimethoxyphenethyl analog **18**, combination of the 4-phenol and 3-methoxy substituents led to potent inhibition activity (**20**, $IC_{50} = 0.035 \mu M$).

We obtained a crystal structure of **7** bound in the ATP binding site of Sky (Fig. 1). The *N*-(3-aminopropyl)-butyrolactam sidechain is oriented towards solvent, while the 2-aminopyrimidine-5-carboxamide core forms three hydrogen bond contacts with the

Pro594 carbonyl and the Met596 amide NH and carbonyl in the hinge region. The hydrogen bond between the 5-carboxamide NH and the Met596 carbonyl is enforced by an intramolecular hydrogen bond between the 4-amino NH and amide carbonyl. In our previously reported Sky crystal structure (3QUP),⁸ we observed an orienting interaction of Lys540 and Asp663 with an inhibitor binding directly to Asp663. In this structure, however, the 4-pyridinethyl group is positioned to interrupt the charge-charge contact between Lys540 and Asp663. This interaction is presumably key for the potent inhibitory activity of the 3-methoxyphenyl analog **17** and the phenolic analogs **19** and **20**. The 4-pyridinethyl group of **7** does not occupy the Ala571 subpocket of the Sky ATP binding site. Previous reports from our group have demonstrated that fill-

Table 2
Heatmap of kinase selectivity for selected compounds^a

Kinases Screened	18	29	31	32
AK1	Green	Green	Green	Green
AKT1	Green	Green	Green	Green
AuroraA	Green	Green	Green	Green
BDK	Green	Green	Green	Green
CEK2/cyclinA	Green	Green	Green	Green
CHK1	Green	Green	Green	Green
CHK2	Green	Green	Green	Green
CHK2	Green	Green	Green	Green
CKI-4/6	Green	Green	Green	Green
EGFR	Green	Green	Green	Green
FGFR1	Green	Green	Green	Green
GSK3- α	Green	Green	Green	Green
IKK- α	Green	Green	Green	Green
IKK- β	Green	Green	Green	Green
IKK- γ	Green	Green	Green	Green
LOK	Green	Green	Green	Green
MAPK1/ERK2	Green	Green	Green	Green
MAPKAPK2	Green	Green	Green	Green
PAR4	Green	Green	Green	Green
PKA	Green	Green	Green	Green
PKB	Green	Green	Green	Green
PKC- α	Green	Green	Green	Green
PKC- δ	Green	Green	Green	Green
PKC- ζ	Green	Green	Green	Green
PKC- η	Green	Green	Green	Green
PKC- θ	Green	Green	Green	Green
PKC- ι	Green	Green	Green	Green
PKC- κ	Green	Green	Green	Green
PKC- λ	Green	Green	Green	Green
PKC- μ	Green	Green	Green	Green
PKC- ν	Green	Green	Green	Green
PKC- ξ	Green	Green	Green	Green
PKC- ω	Green	Green	Green	Green
PKC- γ	Green	Green	Green	Green
PKC- δ	Green	Green	Green	Green
PKC- ϵ	Green	Green	Green	Green
PKC- ζ	Green	Green	Green	Green
PKC- η	Green	Green	Green	Green
PKC- θ	Green	Green	Green	Green
PKC- ι	Green	Green	Green	Green
PKC- κ	Green	Green	Green	Green
PKC- λ	Green	Green	Green	Green
PKC- μ	Green	Green	Green	Green
PKC- ν	Green	Green	Green	Green
PKC- ξ	Green	Green	Green	Green
PKC- ω	Green	Green	Green	Green
PKC- γ	Green	Green	Green	Green
PKC- δ	Green	Green	Green	Green
PKC- ϵ	Green	Green	Green	Green
PKC- ζ	Green	Green	Green	Green
PKC- η	Green	Green	Green	Green
PKC- θ	Green	Green	Green	Green
PKC- ι	Green	Green	Green	Green
PKC- κ	Green	Green	Green	Green
PKC- λ	Green	Green	Green	Green
PKC- μ	Green	Green	Green	Green
PKC- ν	Green	Green	Green	Green
PKC- ξ	Green	Green	Green	Green
PKC- ω	Green	Green	Green	Green
PKC- γ	Green	Green	Green	Green
PKC- δ	Green	Green	Green	Green
PKC- ϵ	Green	Green	Green	Green
PKC- ζ	Green	Green	Green	Green
PKC- η	Green	Green	Green	Green
PKC- θ	Green	Green	Green	Green
PKC- ι	Green	Green	Green	Green
PKC- κ	Green	Green	Green	Green
PKC- λ	Green	Green	Green	Green
PKC- μ	Green	Green	Green	Green
PKC- ν	Green	Green	Green	Green
PKC- ξ	Green	Green	Green	Green
PKC- ω	Green	Green	Green	Green
PKC- γ	Green	Green	Green	Green
PKC- δ	Green	Green	Green	Green
PKC- ϵ	Green	Green	Green	Green
PKC- ζ	Green	Green	Green	Green
PKC- η	Green	Green	Green	Green
PKC- θ	Green	Green	Green	Green
PKC- ι	Green	Green	Green	Green
PKC- κ	Green	Green	Green	Green
PKC- λ	Green	Green	Green	Green
PKC- μ	Green	Green	Green	Green
PKC- ν	Green	Green	Green	Green
PKC- ξ	Green	Green	Green	Green
PKC- ω	Green	Green	Green	Green
PKC- γ	Green	Green	Green	Green
PKC- δ	Green	Green	Green	Green
PKC- ϵ	Green	Green	Green	Green
PKC- ζ	Green	Green	Green	Green
PKC- η	Green	Green	Green	Green
PKC- θ	Green	Green	Green	Green
PKC- ι	Green	Green	Green	Green
PKC- κ	Green	Green	Green	Green
PKC- λ	Green	Green	Green	Green
PKC- μ	Green	Green	Green	Green
PKC- ν	Green	Green	Green	Green
PKC- ξ	Green	Green	Green	Green
PKC- ω	Green	Green	Green	Green
PKC- γ	Green	Green	Green	Green
PKC- δ	Green	Green	Green	Green
PKC- ϵ	Green	Green	Green	Green
PKC- ζ	Green	Green	Green	Green
PKC- η	Green	Green	Green	Green
PKC- θ	Green	Green	Green	Green
PKC- ι	Green	Green	Green	Green
PKC- κ	Green	Green	Green	Green
PKC- λ	Green	Green	Green	Green
PKC- μ	Green	Green	Green	Green
PKC- ν	Green	Green	Green	Green
PKC- ξ	Green	Green	Green	Green
PKC- ω	Green	Green	Green	Green
PKC- γ	Green	Green	Green	Green
PKC- δ	Green	Green	Green	Green
PKC- ϵ	Green	Green	Green	Green
PKC- ζ	Green	Green	Green	Green
PKC- η	Green	Green	Green	Green
PKC- θ	Green	Green	Green	Green
PKC- ι	Green	Green	Green	Green
PKC- κ	Green	Green	Green	Green
PKC- λ	Green	Green	Green	Green
PKC- μ	Green	Green	Green	Green
PKC- ν	Green	Green	Green	Green
PKC- ξ	Green	Green	Green	Green
PKC- ω	Green	Green	Green	Green
PKC- γ	Green	Green	Green	Green
PKC- δ	Green	Green	Green	Green
PKC- ϵ	Green	Green	Green	Green
PKC- ζ	Green	Green	Green	Green
PKC- η	Green	Green	Green	Green
PKC- θ	Green	Green	Green	Green
PKC- ι	Green	Green	Green	Green
PKC- κ	Green	Green	Green	Green
PKC- λ	Green	Green	Green	Green
PKC- μ	Green	Green	Green	Green
PKC- ν	Green	Green	Green	Green
PKC- ξ	Green	Green	Green	Green
PKC- ω	Green	Green	Green	Green
PKC- γ	Green	Green	Green	Green
PKC- δ	Green	Green	Green	Green
PKC- ϵ	Green	Green	Green	Green
PKC- ζ	Green	Green	Green	Green
PKC- η	Green	Green	Green	Green
PKC- θ	Green	Green	Green	Green
PKC- ι	Green	Green	Green	Green
PKC- κ	Green	Green	Green	Green
PKC- λ	Green	Green	Green	Green
PKC- μ	Green	Green	Green	Green
PKC- ν	Green	Green	Green	Green
PKC- ξ	Green	Green	Green	Green
PKC- ω	Green	Green	Green	Green
PKC- γ	Green	Green	Green	Green
PKC- δ	Green	Green	Green	Green
PKC- ϵ	Green	Green	Green	Green
PKC- ζ	Green	Green	Green	Green
PKC- η	Green	Green	Green	Green
PKC- θ	Green	Green	Green	Green
PKC- ι	Green	Green	Green	Green
PKC- κ	Green	Green	Green	Green
PKC- λ	Green	Green	Green	Green
PKC- μ	Green	Green	Green	Green
PKC- ν	Green	Green	Green	Green
PKC- ξ	Green	Green	Green	Green
PKC- ω	Green	Green	Green	Green
PKC- γ	Green	Green	Green	Green
PKC- δ	Green	Green	Green	Green
PKC- ϵ	Green	Green	Green	Green
PKC- ζ	Green	Green	Green	Green
PKC- η	Green	Green	Green	Green
PKC- θ	Green	Green	Green	Green
PKC- ι	Green	Green	Green	Green
PKC- κ	Green	Green	Green	Green
PKC- λ	Green	Green	Green	Green
PKC- μ	Green	Green	Green	Green
PKC- ν	Green	Green	Green	Green
PKC- ξ	Green	Green	Green	Green
PKC- ω	Green	Green	Green	Green
PKC- γ	Green	Green	Green	Green
PKC- δ	Green	Green	Green	Green
PKC- ϵ	Green	Green	Green	Green
PKC- ζ	Green	Green	Green	Green
PKC- η	Green	Green	Green	Green
PKC- θ	Green	Green	Green	Green
PKC- ι	Green	Green	Green	Green
PKC- κ	Green	Green	Green	Green
PKC- λ	Green	Green	Green	Green
PKC- μ	Green	Green	Green	Green
PKC- ν	Green	Green	Green	Green
PKC- ξ	Green	Green	Green	Green
PKC- ω	Green	Green	Green	Green
PKC- γ	Green	Green	Green	Green
PKC- δ	Green	Green	Green	Green
PKC- ϵ	Green	Green	Green	Green
PKC- ζ	Green	Green	Green	Green
PKC- η	Green	Green	Green	Green
PKC- θ	Green	Green	Green	Green
PKC- ι	Green	Green	Green	Green
PKC- κ	Green	Green	Green	Green
PKC- λ	Green	Green	Green	Green
PKC- μ	Green	Green	Green	Green
PKC- ν	Green	Green	Green	Green
PKC- ξ	Green	Green	Green	Green
PKC- ω	Green	Green	Green	Green
PKC- γ	Green	Green	Green	Green
PKC- δ	Green	Green	Green	Green
PKC- ϵ	Green	Green	Green	Green
PKC- ζ	Green	Green	Green	Green
PKC- η	Green	Green	Green	Green
PKC- θ	Green	Green	Green	Green
PKC- ι	Green	Green	Green	Green
PKC- κ	Green	Green	Green	Green
PKC- λ	Green	Green	Green	Green
PKC- μ	Green	Green	Green	Green
PKC- ν	Green	Green	Green	Green
PKC- ξ	Green	Green	Green	Green
PKC- ω	Green	Green	Green	Green
PKC- γ	Green	Green	Green	Green
PKC- δ	Green	Green	Green	Green
PKC- ϵ	Green	Green	Green	Green
PKC- ζ	Green	Green	Green	Green
PKC- η	Green	Green	Green	Green
PKC- θ	Green	Green	Green	Green
PKC- ι	Green	Green	Green	Green
PKC- κ	Green	Green	Green	Green
PKC- λ	Green	Green	Green	Green
PKC- μ	Green	Green	Green	Green
PKC- ν	Green	Green	Green	Green
PKC- ξ	Green	Green	Green	Green
PKC- ω	Green	Green	Green	Green
PKC- γ	Green	Green	Green	Green
PKC- δ	Green	Green	Green	Green
PKC- ϵ	Green	Green	Green	Green
PKC- ζ	Green	Green	Green	Green
PKC- η	Green	Green	Green	Green
PKC- θ	Green	Green	Green	Green
PKC- ι	Green	Green	Green	Green
PKC- κ	Green	Green	Green	Green
PKC- λ	Green	Green	Green	Green
PKC- μ	Green	Green	Green	Green
PKC- ν	Green	Green	Green	Green
PKC- ξ	Green	Green	Green	Green
PKC- ω	Green	Green	Green	Green
PKC- γ	Green	Green	Green	Green
PKC- δ	Green	Green	Green	Green
PKC- ϵ	Green	Green	Green	Green
PKC- ζ	Green	Green	Green	Green
PKC- η	Green	Green	Green	Green
PKC- θ	Green	Green	Green	Green
PKC- ι	Green	Green	Green	Green
PKC- κ	Green	Green	Green	Green
PKC- λ	Green	Green	Green	Green
PKC- μ	Green	Green	Green	Green
PKC- ν	Green	Green	Green	Green
PKC- ξ	Green	Green	Green	Green
PKC- ω	Green	Green	Green	Green
PKC- γ	Green	Green	Green	Green
PKC- δ	Green	Green	Green	Green
PKC- ϵ	Green	Green	Green	Green
PKC- ζ	Green	Green	Green	Green
PKC- η	Green	Green	Green	Green
PKC- θ	Green	Green	Green	Green
PKC- ι	Green	Green	Green	Green
PKC- κ	Green	Green	Green	Green
PKC- λ	Green	Green	Green	Green

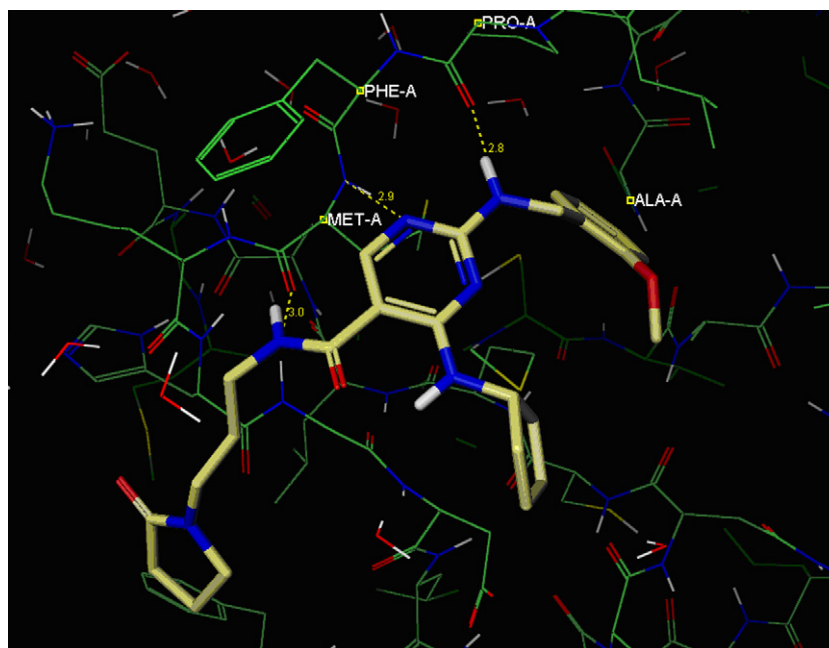


Figure 2. X-ray crystal structure of **29** (yellow stick) bound in the ATP active site of Sky (pdb ID code: 4FF8).¹⁰ The glycine-rich loop has been removed for clarity.

ing the Ala571 pocket is key to achieving selectivity for Sky versus a representative selectivity panel.⁸ As expected from the observed binding mode in the crystal structure, these compounds also inhibited off-target kinases as illustrated by analog **18** which exhibited potent inhibition of Abl, FGFR, and Lck, as well as other members of the HGFR family, Axl, and Mer (Table 2).¹¹

To improve the kinase selectivity, we hypothesized that a shorter and less conformationally constrained sidechain at the pyrimidine 2-position would better fill the Ala571 subpocket. Accordingly, we investigated the SAR of a series of 2-benzylamino analogs (Table 3). The unsubstituted benzyl analog **21** exhibited 2.6-fold reduced inhibitory activity compared to the phenethyl analog **8**. Substitution at the *para*-position resulted in further reduction in activity (analogs **22–24**), indicating that steric constraints were overriding any electronic or lipophilic substituent properties. The 3-Cl analog **25** exhibited improved Sky inhibition activity (IC_{50} = 0.85 μ M), while the 3- CF_3 and 3- CH_3 substituents were detrimental to activity (**26** and **27**, respectively). Electron-withdrawing groups were also not tolerated at the *ortho*-position (**28**, IC_{50} = 1.58 μ M), while the electron-donating 2- OCH_3 group exhibited a sharp improvement in Sky inhibition (**29**, IC_{50} = 0.40 μ M). Further extension of the *ortho*-substituent to a 2-OEt group resulted in further improved inhibition activity (**30**, IC_{50} = 0.215 μ M). The combination of an *ortho*-Cl and *meta*-Cl substituents into a 2,5-disubstitution pattern also resulted in improved activity relative to the monosubstituted chlorobenzyl analogs (**31**, IC_{50} = 0.355 μ M). A crystal structure of analog **29** was obtained that confirmed our hypothesis that a less conformationally mobile benzyl sidechain would fill the Ala571 subpocket (Fig. 2).⁸ As expected from this binding mode, analogs **29** and **31** exhibited excellent kinase selectivity against a panel of 20 & 28 kinases, respectively (Table 2).

All compounds examined thus far exhibited low metabolic stability when incubated with human liver microsomes. While the aromatic ring in the 2-benzylamine sidechain represented a potential site of metabolism, the presence of electron-withdrawing or electron-donating substituents had no effect on the HLM stability. Identification of the metabolites by LC–MS–MS methods indicated

that the primary metabolite was oxidative hydroxylation at the α -carbonyl C atom in the butyrolactam ring. To block this route of metabolism, we converted the butyrolactam ring to an oxazolidin-2-one ring, which exhibited potent Sky inhibition activity (**32**, IC_{50} = 0.070 μ M), but no improvement in HLM stability.

In conclusion, we have discovered a series of Sky inhibitors based on a 2,4-diaminopyrimidine-5-carboxamide template as potential anti-platelet therapy. 2-Phenethylamino analogs with hydrogen-bond accepting groups or phenols at the *para*- or *meta*-positions of the phenyl ring exhibited potent inhibition of Sky, but poor kinase selectivity. 2-Benzylamino analogs with *ortho*- or *meta*-substituents exhibited good inhibition activity and excellent kinase selectivity. These analogs suffer from poor HLM stability. Efforts to improve the HLM stability of this series will be the subject of the following article.

Supplementary data

Supplementary data associated with this article can be found, in the online version, at <http://dx.doi.org/10.1016/j.bmcl.2012.12.013>.

References and notes

- American Heart Association. Heart Disease and Stroke Statistics—2007 Update.
- Cattaneo, M. *Arterioscler. Thromb. Vasc. Biol.* **2004**, *24*, 1980.
- Saller, F.; Burnier, L.; Schapira, M.; Angelillo-Scherrer, A. *Blood Cells Mol. Dis.* **2006**, *36*, 373.
- Angelillo-Scherrer, A.; de Frutos, P. G.; Aparicio, C.; Melis, E.; Savi, P.; Lupu, F.; Arnout, J.; Dewersch, M.; Hoylaerts, M. F.; Herbert, J.-M.; Collen, D.; Dahlbäck, B.; Carmeliet, P. *Nat. Med.* **2001**, *7*, 215.
- Gould, W. R.; Baxi, S. M.; Schroeder, R.; Peng, Y. W.; Leadley, R. J.; Peterson, J. T.; Perrin, L. A. *J. Thromb. Haemost.* **2005**, *3*, 733.
- Nagata, K.; Ohashi, K.; Takano, T.; Arita, H.; Zong, C.; Hanafusa, H.; Mizuno, K. *J. Biol. Chem.* **1996**, *271*, 30022.
- Angelillo-Scherrer, A.; Burnier, L.; Flores, N.; Savi, P.; DeMol, M.; Schaeffer, P.; Herbert, J.-M.; Lemke, G.; Goff, S. P.; Matsushima, G. K.; Earp, H. S.; Vesin, C.; Hoylaerts, M. F.; Plaisance, S.; Collen, D.; Conway, E. M.; Wehrle-Haller, B.; Carmeliet, P. *J. Clin. Invest.* **2005**, *115*, 237.
- Powell, N. A.; Kohrt, J. T.; Filipowski, K. J.; Kaufman, M.; Sheehan, D.; Edmunds, Jeremy J.; Delaney, A.; Wang, Y.; Bourbonais, F.; Lee, D.-Y.; Schwende, F.; Sun,

- F.; Fauman, E.; McConnell, P.; Catana, C.; Chen, H.; Ohren, J.; Perrin, L. A. *Bioorg. Med. Chem. Lett.* **2012**, 22, 190.
9. Baughman, T. A.; Boyce, J. P.; Darwish, I. S.; Howbert, J. J.; Ihle, N. C.; Jackson, R. W.; Jeffrey, S. C.; Maeda, D.; Yager, K. M. U.S. Patent 7,176,310, 2007.
10. Coordinates for the Sky/7 complex (4FEQ) and Sky/29 complex (4FF8) have been deposited at www.rcsb.org.
11. Liu, J.; Yang, C.; Simpson, C.; DeRyckere, D.; Van Deusen, A.; Miley, M. J.; Kireeve, D.; Norris-Drouin, J.; Sather, S.; Hunter, D.; Korboukh, V. K.; Patel, H. S.; Janzen, W. P.; Machius, M.; Johnson, G. L.; Earp, H. S.; Graham, D. K.; Frye, S. V.; Wang, X. *ACS Med. Chem. Lett.* **2012**, 3, 129.